5th International Conference on Control Engineering&Information Technology (CEIT-2017)
Proceeding of Engineering and Technology –PET
Vol.32 pp.21-26

DFIG Analysis under Grid Voltage Sags Based on Symmetrical Components

Meriem Ghodbane-Cherif[#1], Sondes Skander-Mustapha[#*2], Ilhem Slama-Belkhodja[#3], Azeem Khan[&4]

[#] *Université de Tunis El Manar, Ecole Nationale d'Ingénieurs de Tunis, LR11ES15 Laboratoire de Systèmes Electriques, 1002, Tunis, Tunisie*

** Université de Carthage, Ecole Nationale d'Architecture et d'Urbanisme, 2026, Sidi Bou Said, Tunisie*

[1]meriem.ghodbane.enit.utm.tn

[2]sondes.skander@enit.utm.tn

[3]ilhem.slamabelkhodja@enit.utm.tn

[&] *Department of Electrical Engineering, University of Cape Town Private Bag, Rondebosch, 7701Cape Town, South Africa*

[4]azeem.khan@uct.ac.za

Abstract—**Due to its variable speed wind operation and cost effectiveness, doubly fed induction generator (DFIG) is extensively used in wind power generation. However, DFIG based variable speed wind system (VSWS) is vulnerable to power grid disturbances and faults. In another hand, grid code requirements (GCR) imposed by the grid operators are becoming more severe to ensure the low voltage ride through (LVRT). Several control methods are proposed in the bibliography to meet the grid code requirements under fault conditions. In the present study, an approach based on symmetrical components theory in time domain is proposed for a grid connected wind system based on DFIG to analyse its performances under faulty operation. A theoretical analysis is given to explain the proposed method, then, the DFIG behaviour under symmetrical and asymmetrical grid faults is investigated. Simulation has been carried out under PSIM software and simulation results are discussed to provide some comments and conclusions.**

***Keywords*— Wind system, doubly-fed induction generator, symmetrical components, Voltage sags, field -oriented control.**

I. INTRODUCTION

Recently, due to the rise in the demand for electrical energy and the necessity to reduce CO_2 emissions, the attention soars towards green energy integration, especially wind power. Among the wind systems, variable speed wind systems based on doubly fed induction generator (DFIG) have drawn considerable attention because of its partially rated converters and its ability to operate with decoupled active and reactive power control [1]-[5]. It has reduced size, weight, losses and, consequently, cost compared to full power converter based system. However, DFIG based wind systems are very sensitive to grid disturbances, especially to voltage sags [6]. Since the low voltage ride through (LVRT) fulfillment for wind turbines has become a major requirement all around the world, the wind farms connected to grid are required to stay connected even during symmetrical or asymmetrical voltage sags. Several researches have been carried out to improve the LVRT capacity of DFIG [7]-[10]. Wind systems are also expected to support the grid, through reactive power generation, during system faulty period and recovers on to maintain the grid stability [11]. The analysis and control of the DFIG under normal grid conditions and grid disturbances have been widely treated in the literature [12]-[16]. Many authors have used the symmetrical components theory for detection and characterization of voltage sags [17]-[18].

This paper deals with the behavior analysis of a DFIG based wind system under symmetrical and asymmetrical voltage sags using symmetrical components theory [19]. The paper is structured as follows. Section II deals with the modelling of grid connected variable speed wind system based on DFIG in d-q Park reference frame. Section III describes the proposed control strategies for back-to-back converters. In section IV, instantaneous symmetrical components theory has been introduced to analyse grid voltage sags. Section V describes the faulty behaviour of the DFIG and the impact of symmetrical and asymmetrical sags on its operating performance. Section VI concludes the paper.

II. SYSTEM DESCRIPTION AND DFIG MODELLING

The studied system is a grid connected variable speed wind system based on DFIG. The basic configuration of the wind system is composed, as shown in Fig.1, of blades, mechanical shaft system, gear-box, DFIG, back-to-back converters and their control system. The DFIG stator is directly connected to the grid and the rotor is linked to the grid through back-to-back converters. These controlled converters allow Bi-directional power flow between DFIG and the grid. A common DC-link capacitor is coupled between the two converters to keep the voltage ripples in the dc-link within an acceptable range. The purpose of the rotor side converter (*RsC*) is to control both the active and reactive stator powers. The main objective of the grid side converter (*GsC*) control is to maintain a constant DC-link voltage, in addition of the control

Copyright IPCO-2017
ISSN 2356-5608

of the power exchanged between the rotor windings and the grid. An inductor filter interfaces the *GsC* with the grid.

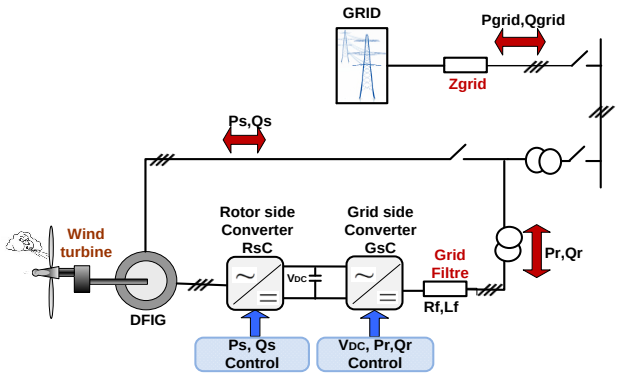

Fig.1 Variable speed wind system based on DFIG

The dynamic DFIG model in the *d-q* synchronous rotating reference frame is given by the following equations:

$$\bar{v}_{s(d,q)} = v_{sd} + jv_{sq} = R_s \bar{i}_{s(d,q)} + \frac{d\bar{\varphi}_{s(d,q)}}{dt} + j\omega_s \bar{\varphi}_{s(d,q)} \quad (1)$$

$$\bar{v}_{r(d,q)} = v_{rd} + jv_{rq} = R_r \bar{i}_{r(d,q)} + \frac{d\bar{\varphi}_{r(d,q)}}{dt} + j\omega_r \bar{\varphi}_{r(d,q)} \quad (2)$$

Where R_s and R_r are, respectively, the stator and rotor phase resistances, v_{sd}, v_{sq}, v_{rd} and v_{rq} are, respectively, the *d* and *q*-axes components of stator and rotor voltages respectively; $\bar{i}_{s(d,q)}$ and $\bar{i}_{r(d,q)}$ are the *d* and *q*-axes components of stator and rotor currents respectively; $\bar{\varphi}_{s(d,q)}$ and $\bar{\varphi}_{r(d,q)}$ are electromagnetic flux components; ωs and ωr are, respectively, the stator and rotor electrical angular frequencies.

The active and reactive powers provided for the grid through the stator are defined as:

$$P_s = v_{sd} i_{sd} + v_{sq} i_{sq} \quad (3)$$

$$Q_s = v_{sq} i_{sd} - v_{sd} i_{sq} \quad (4)$$

III. System Control

As shown in Fig.1, the DFIG is fed from both the stator side and the rotor side. The control of the system is assured by the back-to-back converters which consist of two four-quadrant PWM converters: the *RsC* and the *GsC*. A vector control technique is developed for each converter.

A. Rotor side converter control strategy

The proposed control structure is illustrated in Fig.2 The theory of flux oriented control (FOC) has been developed for the *RsC*. This choice is made because under the stator flux orientation, the active and reactive powers are decoupled and can be controlled via only rotor currents. In other words, rotor current direct component and quadrature component can be commanded to control stator reactive and active powers respectively. First, the relationship between the rotor currents and the stator powers is obtained to generate the rotor current references. Then, the rotor currents are regulated through closed control loops using proportional integrator PI regulators. The outputs of the two current controllers are compensated by the corresponding cross-coupling terms to form the total voltage signals to apply to the SVM module. This module generates the gate control signals to drive the *RsC*.

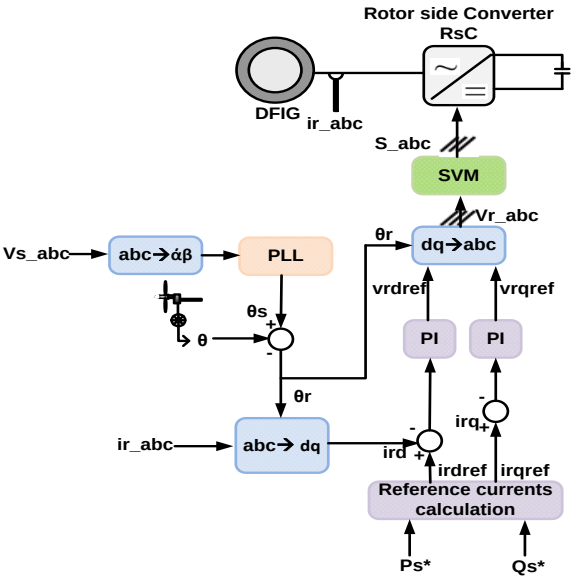

Fig.2 RsC proposed control

The flux orientation, as shown in Fig.3, is chosen such as the flux is aligned with *d*-axis which means *q*-axis flux component $\varphi_{sq} = 0$.

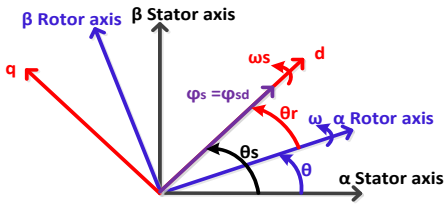

Fig.3 Flux orientation

In this synchronous reference frame, the stator and rotor fluxes are related to the current by the following equations:

$$\varphi_{sd} = L_s i_{sd} + M_{sr} i_{rd} \quad (5)$$

$$\varphi_{rd} = L_r i_{rd} + M_{sr} i_{sd} \quad (6)$$

$$\varphi_{rq} = L_r i_{rq} + M_{sr} i_{sq} \quad (7)$$

Where L_s and L_r are, respectively, the stator and rotor phase inductances, M_{sr} is the magnetizing inductance of the DFIG. Rotor current references for regulation loops are expressed by (8) and (9) under the assumption that the effect of the stator and the rotor resistances are neglected:

$$i_{rdref} = \frac{L_s}{M_{sr} v_{sq}} \left(\frac{v_{sq} \varphi_{sd}}{L_s} - Q_{sref} \right) \quad (8)$$

$$i_{rqref} = -\frac{L_s}{M_{sr} v_{sq}} P_{sref} \quad (9)$$

B. Grid side converter control strategy

The proposed control structure for the *GsC* is depicted in Fig.4. The theory of voltage oriented control (VOC) has been developed for the *GsC*. The vector orientation is chosen such as the grid voltage vector is aligned with the *q*-axis. The *GsC* is controlled using two cascade loops. The outer control loop controls the DC-link voltage V_{DC} and the reactive power. The inner loop controls the line currents $i_{L(d,q)}$. PI controllers have been used for regulation.

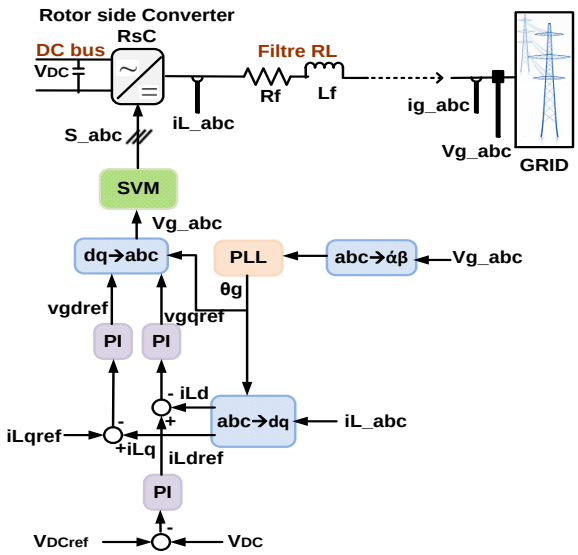

Fig.4 GSC proposed control

In the rotational reference frame linked to the grid voltage, the line voltages v_{Ld} and v_{Lq} are given by the following equations:

$$v_{Ld} = R_f i_{Ld} + L_f \frac{di_{Ld}}{dt} - \omega_g i_{Lq} + v_{gd} \quad (10)$$

$$v_{Lq} = R_f i_{Lq} + L_f \frac{di_{Lq}}{dt} + \omega_g i_{Ld} + v_{gq} \quad (11)$$

Where R_f and L_f are the filter resistance and inductance respectively, $i_{L(d,q)}$ and $v_{g(d,q)}$ are the *d* and *q*-axes components of the line currents and grid voltages respectively and ω_g is the grid angular frequency. The *q*-axis grid voltage component $v_{gq} = 0$ since the rotational reference frame is linked to the grid voltage. The equations (10) and (11) allow the PI controllers design.

IV. Voltage Sags Analysis Based on Symmetrical Components Decomposition

A. Symmetrical Components Theory

Instantaneous symmetrical components theory has been introduced by C.L.Fortescue in [19]. This theory is used to analyse three-phase systems under symmetrical and asymmetrical conditions. According to C.L.Fortescue, any asymmetrical system of n phasors can be decomposed into n-1 balanced phase systems of different phase sequence and one zero sequence system. In each sequence, all phasors are of equal magnitude and cophasial. The decomposition results for a three-phase system are known as positive, negative and zero sequence components. Considering a three-phase system (X_a, X_b, X_c), it can be expressed in terms of the symmetrical components as:

$$\begin{pmatrix} X_a \\ X_b \\ X_c \end{pmatrix} = \begin{pmatrix} X_{ap} \\ X_{bp} \\ X_{cp} \end{pmatrix} + \begin{pmatrix} X_{an} \\ X_{bn} \\ X_{cn} \end{pmatrix} + \begin{pmatrix} X_{ao} \\ X_{bo} \\ X_{co} \end{pmatrix} \quad (12)$$

Where subscripts "*p*", "*n*" and "*o*" denote the positive, negative and zero sequence respectively. The positive, negative and the zero sequences are defined as follow:

$$\begin{pmatrix} X_{ap} \\ X_{bp} \\ X_{cp} \end{pmatrix} = \frac{1}{3} \begin{pmatrix} 1 & a^2 & a \\ a & 1 & a^2 \\ a^2 & a & 1 \end{pmatrix} \begin{pmatrix} X_a \\ X_b \\ X_c \end{pmatrix} \quad (13)$$

$$\begin{pmatrix} X_{an} \\ X_{bn} \\ X_{cn} \end{pmatrix} = \frac{1}{3} \begin{pmatrix} 1 & a & a^2 \\ a^2 & 1 & a \\ a & a^2 & 1 \end{pmatrix} \begin{pmatrix} X_a \\ X_b \\ X_c \end{pmatrix} \quad (14)$$

$$X_{ao} = X_{bo} = X_{co} = \frac{1}{3}\left(X_a + X_b + X_c\right) \quad (15)$$

Where the operator "*a*" is defined by a $=1 \angle 120°$ and $a^2 = 1 \angle 240°$.

It is obvious from equations (14) and (15) that the instantaneous value of the negative and zero sequences are zero when all the three phases are balanced.

B. Voltage Sags Analysis

To illustrate the symmetrical component use for analysis of signals, the decomposition of symmetrical and asymmetrical voltage sags have been simulated under PSIM software and simulation results are given in TABLE I. In the first column, simulation results have been obtained for a 30% symmetrical voltage sag (three-phase sag). In the second column, simulation has been conducted for a 30% asymmetrical voltage sag (single phase sag). A 400V variable voltage source represents the 50 Hz grid. Per unit values are used for the waveforms with a base voltage of 400V.

Waveforms of TABLE I show neither negative nor zero sequence, under symmetrical sag, as expected. However,

during this type of sag, instantaneous value of the positive sequence decreases with the sag magnitude.
The change in the instantaneous value of the negative and zero sequences of the three-phase source, in addition of the decrease in the instantaneous value of the positive sequence, confirms asymmetrical sag occurrence.
These results confirm that symmetrical components can be easily used for voltage sags detection.

TABLE I
Voltage sags decomposition

	Symmetrical sag	Asymmetrical sag
	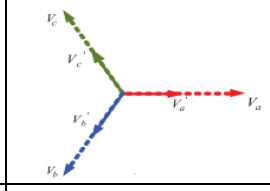	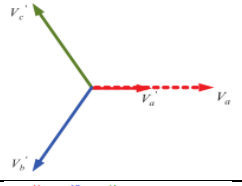
	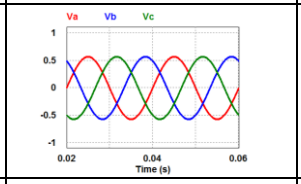	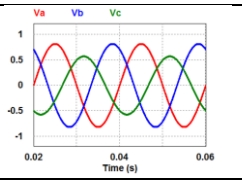
Positive sequence	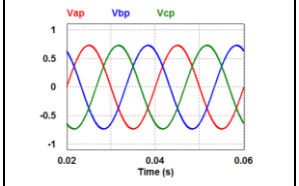	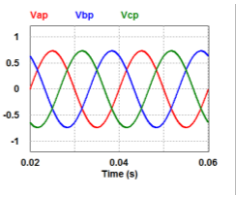
Negative sequence	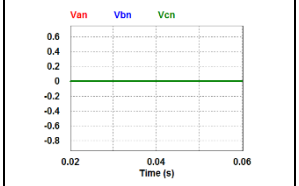	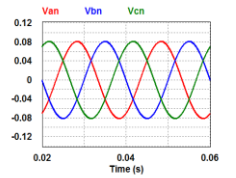
Zero sequence	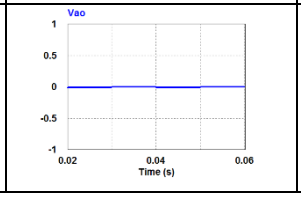	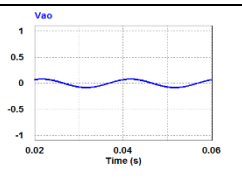

V. DFIG Behaviour During Voltage Sag Based on Symmetrical Components Theory

In this section, to study the DFIG behaviour during voltage dips, the use of symmetrical components for the analysis of the DFIG operation under symmetrical and asymmetrical voltage sags has been illustrated.

Decomposition of the voltages and currents in positive and negative sequences and their introduction in stator powers expressions, equations (3) and (4), leads to the following stator power expressions:

$$\begin{cases} P_s = P_{so} + P_{s\cos}\cos(2\omega_g t) + P_{s\sin}\sin(2\omega_g t) \\ Q_s = Q_{so} + Q_{s\cos}\cos(2\omega_g t) + Q_{s\sin}\sin(2\omega_g t) \end{cases} \quad (16)$$

Where P_{so}, P_{cos}, P_{sin}, Q_o, Q_{cos}, Q_{sin} are given by the following matrix:

$$\begin{pmatrix} P_{so} \\ Q_{so} \\ P_{s\cos} \\ P_{s\sin} \\ Q_{s\cos} \\ Q_{s\sin} \end{pmatrix} = \begin{pmatrix} v_{sdp} & v_{sqp} & v_{sdn} & v_{sqn} \\ v_{sqp} & -v_{sdp} & v_{sqn} & -v_{sdn} \\ v_{sdn} & v_{sqn} & v_{sdp} & v_{sqp} \\ v_{sqn} & -v_{sdn} & -v_{sqp} & v_{sdp} \\ v_{sqn} & -v_{sdn} & v_{sqp} & -v_{sdp} \\ -v_{sdn} & -v_{sqn} & v_{sdp} & v_{sqp} \end{pmatrix} \cdot \begin{pmatrix} i_{sdp} \\ i_{sqp} \\ i_{sdn} \\ i_{sqn} \end{pmatrix} \quad (17)$$

Zero sequence components are neglected, since the DFIG is considered three-phase three-wire in this paper.
Oscillations in the powers can easily be analyzed by using the equations (16) and (17). If stator voltages are balanced, no negative sequence appears in the powers, therefore, v_{sdn}, v_{sqn}, i_{sdn}, and i_{sqn} are null. Consequently, P_{scos}, P_{ssin}, Q_{scos} and Q_{ssin} coefficients are equal to zero and there will be no oscillations in the powers. However, if sag occurs, the stator voltages will be unbalanced and these coefficients will not be null. Subsequently, power ripples appear at twice the grid frequency.
Since the electromagnetic torque is related to the stator power by the following equation:

$$T_{em} = P_s \frac{p}{\omega_s} \quad (18)$$

Where p is the number of pairs of poles.
Stator power oscillations lead to torque ripples. That is why it is interesting to analyze oscillations in the powers. It is obvious that the flux causes oscillations at the grid frequency in the torque and stator powers. Additional oscillations at twice the grid frequency, in the case of asymmetrical sags, are caused by the negative sequence.

Simulation results have been obtained for 4kW system with 4-pole doubly fed induction machine Its parameters are reported in TABLE II of the appendix. In Fig.5 and Fig.6, DFIG responses under a 30% asymmetrical grid voltage sag (single phase sag) are presented. The sag occurs at t=0.2 s.
Per unit values are used for the waveform and the base value for power is 4kVA.

Fig.5 (a), (b), (c) and (d) illustrate stator active power P_s and the coefficients of its various components P_{so}, P_{scos}, P_{ssin}, respectively, while Fig.6 (a), (b), (c) and (d) illustrate stator reactive power Q_s and the coefficients of its various components Q_{so}, Q_{scos}, Q_{ssin} respectively.

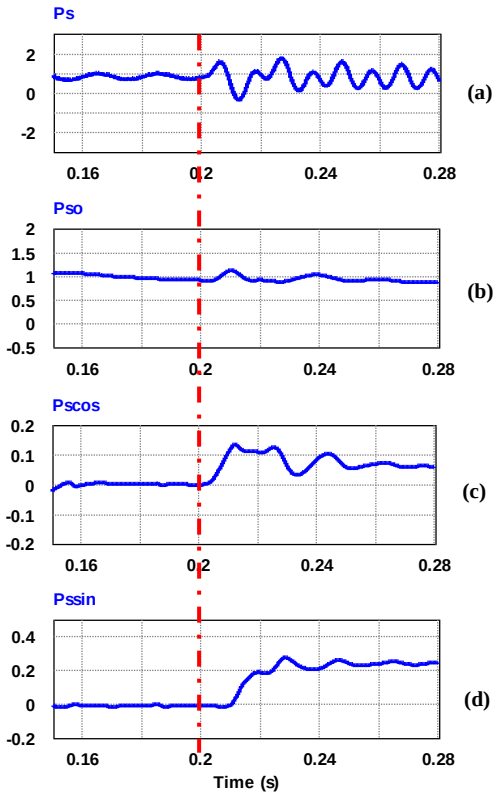

Fig.5 Active power for DFIG faulty operation

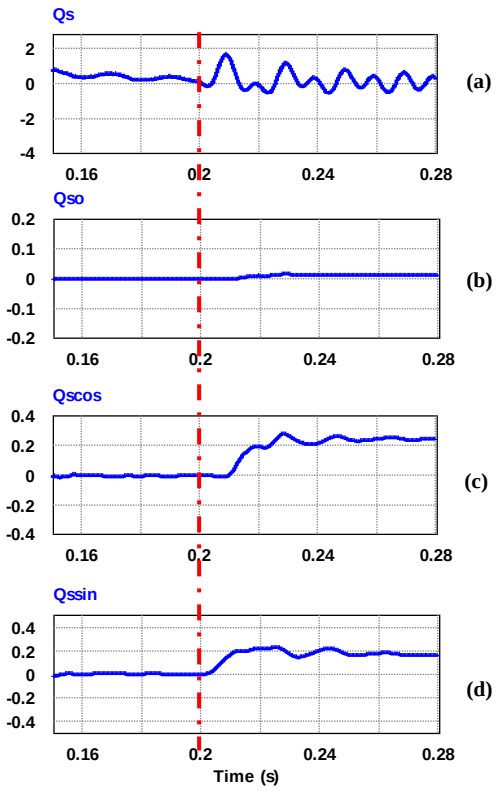

Fig.6 Reactive power for DFIG faulty operation

The simulations results validate the theoretical analysis: The different simulation results obtained show that the stator power, in absence of sags, will be constant and equal to the value of P_{so}. The average value of the reactive power will also be equal to the value of Q_{so}. However, if asymmetrical sag occurs, an alternating power will appear: P_{scos}, P_{ssin}, Q_{scos}, Q_{ssin}).

VI. Conclusions

In this work, the dq dynamic model of the DFIG has been presented, before continuing with the analysis of the grid connected variable speed wind system based on DFIG and addresses its control. The innovative contribution of this work lies in an original method for DFIG fault behaviour analysis. This method has been used time domain symmetrical components which decompose the steady-state phasors of three-phase voltage and current systems into a set of positive, negative and zero sequences. The findings of this study offer deep understanding of the faulty behaviour of the DFIG and the impact of symmetrical and asymmetrical sags on its operating performance. Indeed, the voltage sag will cause transmission line voltage unbalance as well as powers fluctuation akin to double power grid frequency. This severely influences the performance of the wind power system and its safe operation. Moreover, this proposed method can be applied to detect sags.

Appendix

TABLE II

DFIG parameters for the case study

Description	Symbol	Value	Unit
Rated power	P	4	kW
Rated stator voltage	V_s	400	V
Rated rotor voltage	V_r	130	V
Rated stator current	I_s	8.4	A
Rated rotor current	I_r	19	A
Frequency	f_s	50	Hz
Stator resistance	R_s	3.63	W
Rotor resistance	R_r	0.49	W
Stator cyclic inductance	L_s	0.748	H
Rotor cyclic inductance	L_r	0.027	H
Mutual cyclic inductance	M_{sr}	0.139	H

ACKNOWLEDGMENT

This work was supported by the Tunisian Ministry of High Education and Research under Grant LSE-ENIT-LR 11ES15 and the Tuniso-South African Collaboration project “Generator Test Platform for Assessing the Impact of Wind Integration and Power Quality Issues”.

References

[1] E. Aydin, A. Polat, L. T. Ergene “Vector Control of DFIG in Wind Power Applications,” International Conference on Renewable Energy Research and Applications, vol. 5, pp. 478-483, no. 1, Nov.20-23, 2016.

[2] J. Faiz and S. M. M. Moosavi, “Eccentricity fault detection – From induction machines to DFIG — A review,” Renew. Sustain. Energy Rev., vol. 55, pp. 169–179, 2016.

[3] G. P. Prajapat, N. Senroy and I. N. Kar, “Wind Turbine Structural Modeling Consideration for Dynamic Studies of DFIG based System,” , IEEE Transactions on Sustainable Energy, vol. 3029, pp. 1–10, 2017.

[4] P. Cheng, H. Nian, C. Wu, and Z. Q. Zhu, “Direct Stator Current Vector Control Strategy of DFIG Without Phase-Locked Loop During Network Unbalance,” IEEE Transactions On Power Electronics, vol. 32, no. 1, pp. 284–297, 2017.

[5] Y.-K. Wu and W.-H. Yang, “Different Control Strategies on the Rotor Side Converter in DFIG-based Wind Turbines,” Energy Procedia, vol. 100, pp. 551–555, 2016.

[6] N. Kumar, T. R. Chelliah, and S. P. Srivastava, “Analysis of doubly-fed induction machine operating at motoring mode subjected to voltage sag,” Engineering Science and Technology, an International Journal , pp. 1–15, 2016.

[7] M. Ezzat, M. Benbouzid, S. M. Muyeen, and L. Harnefors, “Low-voltage ride-through techniques for DFIG-based wind turbines: state-of-the-art review and future trends,” IECON - 39th Annu. Conf. IEEE Indus. Electron. Soc., pp. 7681–7686, 2013.

[8] X. Zhao, J. M. Guerrero, M. Savaghebi, J. C. Vasquez, X. Wu, and K. Sun, “Low Voltage Ride-Through Operation of Power Converters in Grid-Interactive Microgrids by Using Negative-Sequence Droop Control,” IEEE Trans. Power Electron., vol. 32, no. 4, pp. 3128–3142, April 2016.

[9] A. R. Ann, P. Kaliannan, and U. Subramaniam, “Improved fault ride through capability of DFIG based wind turbines using synchronous reference frame control based dynamic voltage restorer,” *ISA Trans.*, 2017.

[10] S. Tohidi and B. Mohammadi-ivatloo, “A comprehensive review of low voltage ride through of doubly fed induction wind generators,” vol. 57, pp. 412–419, 2016.

[11] M. E. Hossain, “A new approach for transient stability improvement of a grid-connected doubly fed induction generator–based wind generator,” Wind Eng., pp.1-15, 2017.

[12] P. Pura and G. Iwanski, “Direct power control based torque oscillations cancellation in doubly fed induction generator operating with unbalanced grid,” Proc 10th Int. Conf. Compat. Power Electron. Power Eng. CPE-POWERENG 2016, pp. 180–185, 2016.

[13] G. Junghare, P. Debre, and A. Kadu, “Analysis ofDoubly Fed Induction Generator Interconnected with Grid under Normal and Abnormal Condition,” 1st IEEE International Conference on Power Electronics. Intelligent Control and Energy Systems (ICPEICES-2016) Analysis, 2016.

[14] T. K. Das, “Counteracting the Effects of Symmetrical and Asymmetrical Voltage Sags on DFIG-Based Wind Power Systems,” pp. 79–84, Proceedings of the 2016 International Conference on Advanced Mechatronic Systems, Melbourne, Australia, November 30 - December 3, 2016

[15] P. Tourou and C. Sourkounis, “Review of control strategies for DFIG-based wind turbines under unsymmetrical grid faults,” *2014 9th Int. Conf. Ecol. Veh. Renew. Energies, EVER* , 2014.

[16] R. Kumar, B. Singh, and D. T. Shahani, “Symmetrical Components-Based Modified Technique for Power-Quality Disturbances Detection and Classification,” IEEE Trans. Ind. Appl., vol. 52, no. 4, pp. 3443–3450, 2016.

[17] J. Suma and M. K. Mishra, “Instantaneous symmetrical component theory based algorithm for characterization of three phase distorted and unbalanced voltage sags,” Proc. IEEE Int. Conf. Ind. Technol., pp. 845–850, 2013.

[18] A. S. Hati and T. K. Chatterjee, “Symmetrical component filter based on line condition monitoring instrumentation system for mine winder motor,” *Meas. J. Int. Meas. Confed.*, vol. 82, pp. 284–300, 2016.

[19] C. L. Fortescue, “Method of Symmetrical Coordinates Aplied to the Solution of Poliphase Networks,” *Trans. AIEE*, vol. 37, pp. 1027–1140, 1918.